CHEMISTRY
A European Journal

A Journal of
ChemPubSoc Europe

Title: Synthesis of a New Microporous Zincosilicate with CHA Zeolite Topology as Efficient Platforms for Ion-Exchange of Divalent Cations

Authors: Natsume Koike, Kenta Iyoki, Sye Hoe Keoh, Watcharop Chaikittisilp, and Tatsuya Okubo

To be cited as: *Chem. Eur. J.* 10.1002/chem.201705277

Link to VoR: http://dx.doi.org/10.1002/chem.201705277

Supported by
ACES

WILEY-VCH

WILEY-VCH

COMMUNICATION

Synthesis of a New Microporous Zincosilicate with CHA Zeolite Topology as Efficient Platforms for Ion-Exchange of Divalent Cations

Natsume Koike, Kenta Iyoki, Sye Hoe Keoh, Watcharop Chaikittisilp,* and Tatsuya Okubo*[a]

Abstract: There is growing interest to develop zeolite materials capable of stabilizing divalent cations such as Cu^{2+}, Fe^{2+}, and Ni^{2+} for catalytic applications. Herein, we describe for the first time the synthesis of a new microporous zincosilicate with CHA zeolite topology by particularly focusing on the mixing procedures of the raw materials to prevent the precipitation of zinc oxides/hydroxides and the formation of impure phases. The obtained zincosilicate CHA products possess remarkably higher ion-exchange ability for catalytically useful, divalent cations, demonstrated here using Ni^{2+} as an example, compared to that of aluminosilicate and zincoaluminosilicate analogs. We anticipate that these zincosilicate CHA materials can be an efficient platform for several important catalytic reactions. In addition, the present finding would provide a general guideline for effective substitution of other heteroatoms into the zeolite frameworks.

Diversification of the framework elements of inorganic framework materials by heteroatom substitution is of great scientific and technological significance because the physicochemical properties of the materials can be substantially altered by such heteroatoms, thereby providing specific functionality for particular applications. As one of the representative classes of the inorganic framework materials, zeolites, crystalline microporous aluminosilicates, have been indispensable for several applications as adsorbents, ion-exchangers, separation membranes and catalysts.[1,2] Recently, small-pore zeolites defined as the zeolites having the pore openings limited by 8 tetrahedral atoms (8-ring, 8*r*) have received particular attention because they have exhibited excellent performance in several important applications, for example, as catalysts for methanol-to-olefin (MTO) and ethene-to-propene (ETP) reactions, and as adsorbents and membranes for gas separations.[3–5] Among several small pore zeolites, CHA-type zeolite possessing a large *cha* cage cavities with 8*r* openings has been intensively studied. Both aluminosilicate and silicoaluminophosphate versions of the CHA materials (i.e., SSZ-13 and SAPO-34, respectively) are efficient catalysts for MTO and ETP reactions, for which they have been commercialized or close to be commercialized.[4]

Divalent cation-exchanged zeolites have recently shown great promise in several new applications relevant to energy and environment. For example, Cu^{2+}- and Fe^{2+}-exchanged zeolites have proven to be efficient catalysts for selective catalytic reduction (SCR) of NO_x and methane conversions.[6–9] For such reactions, the local environments of divalent cations remarkably affect the catalytic activity.[8–11] For example, monocopper sites in small-pore zeolites were reported to be active sites for SCR of NO_x.[7,10] Note that in larger pore zeolites di- and trinuclear metal oxo-clusters can also catalyze such reactions through different catalytic mechanisms.[9,11,12] For aluminosilicate zeolites to stabilize the active monomeric sites of divalent metals, two Al with close proximity (e.g., Al paired configuration Al–O–(Si–O)$_n$–Al (n = 1, 2) in 6*r*), are required because isomorphous substitution of Al(III) for Si(IV) in the zeolite framework generates only one anionic charge per Al atom.[13] On the other hand, isolated Al is suitable for stabilization of oxo-species of divalent cations, which are sometimes undesired.[7,14] In addition, isolated Al sites can remain as Brønsted acid sites when counterbalanced by protons and hence cause side reactions and catalyst deactivation.[15] It was reported that, in the case of high-silica CHA zeolites, the isolated Al exists dominantly.[16] Although the fraction of paired Al in the CHA zeolites can be increased by carefully tuning the synthesis conditions, the density of paired Al cannot be increased more than that found in zeolites with random Al distribution.[16]

On the contrary, isomorphous substitution of Zn(II) for Si(IV) in the zeolite framework can generate two anionic charges per Zn atom, making zincosilicate zeolite-like materials a promising platform for stabilization of divalent cations.[15] However, a number of available zincosilicates are quite limited to only few zeolite frameworks.[17–19] In addition, Zn is easily precipitated as oxides or hydroxides in basic media during hydrothermal synthesis,[20] akin to other metal-substituted zeolite-like materials. Recently, synthesis of zincoaluminosilicate CHA having both Al and Zn in their frameworks was reported.[21] In this case, a large amount of Al is necessary for directing the crystallization of CHA. Still, synthesis of zincosilicate CHA without any Al in the framework is desired because framework Al can sometime lead to undesired side reactions.[15]

Aluminosilicate CHA zeolites naturally occur as a mineral and can be synthesized without using any organic structure-directing agent (OSDA) in Al-rich aluminosilicate compositions. The Si-rich CHA zeolite, known as SSZ-13, was successfully synthesized using *N*,*N*,*N*-trimethyl-1-adamantylammonium hydroxide (TMAdaOH) as an OSDA.[22] Recently, the synthesis of silicate-based CHA materials has advanced beyond the aluminosilicate composition to, for example, titanosilicate[23] and stannosilicate,[24]

---

[a] N. Koike, Dr. K. Iyoki, Dr. S. H. Keoh, Dr. W. Chaikittisilp, Prof. Dr. T. Okubo
Department of Chemical System Engineering
The University of Tokyo
7-3-1 Hongo, Bunkyo-ku, Tokyo 113-8656 (Japan)
E-mail: watcha@chemsys.t.u-tokyo.ac.jp
okubo@chemsys.t.u-tokyo.ac.jp

Supporting information for this article is given via a link at the end of the document.

which have been achieved in fluoride media. In their syntheses, balanced reaction (hydrolysis/dissolution and condensation) rates of Si source and metal precursors were reported to be of significance.[23,24]

We report herein for the first time the synthesis of a new microporous zincosilicate with CHA zeolite topology. To prevent the precipitation of extraframework zinc oxides/hydroxides, we pay particular attention to the mixing procedures of the raw materials prior to hydrothermal treatment. For the successful synthesis of zincosilicate CHA, the initial state of Zn species in a basic solution is very crucial. In a typical procedure (see procedure (i) in Figure 1a), lithium hydroxide monohydrate was dissolved in distilled water and fumed silica was then added to the solution. After stirring for 2 h, a semitransparent suspension is obtained. In another vessel, anhydrous zinc acetate was added to an aqueous solution of TMAdaOH and stirred for 5 min to obtain a clear solution. The amounts of water in the silica suspension and the Zn solution are identical. The Zn solution was then added to the silica suspension and further stirred for 5 min. The molar ratio of the final mixture was SiO_2: 0.03 ZnO: 0.42 TMAdaOH: 0.08 LiOH: 30 H_2O. After hydrothermal treatment at 150 °C under a static condition for a week, a highly crystalline CHA product was obtained, hereafter referred to as Zn-CHA1 (Figure 1b).

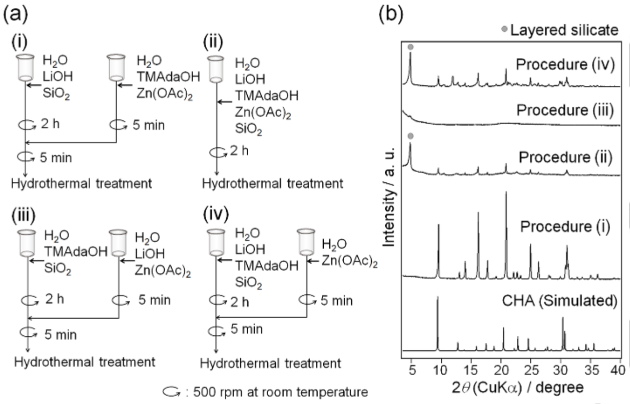

Figure 1. (a) Schemes of mixing procedures of synthetic mixtures prior to hydrothermal treatment (see experimental details in the Supporting Information). (b) Powder XRD patterns of products obtained via different mixing procedures (i)–(iv) after hydrothermal treatment at 150 °C for 7 days under a static condition.

Interestingly, when the synthetic mixtures were prepared in different ways (procedures (ii)–(iv) in Figure 1a), the products were either amorphous solid or the mixture of layered silicate and CHA (see Figure 1b). Figure S2 in the Supporting Information shows SEM images of the product obtained from the different procedures (i)–(iv). The CHA product obtained from the procedure (i) was uniform, cubic particles with a size of ca. 6 μm. On the other hand, the layered material-like particles were observed in the product prepared by the procedure (ii) with only a small portion of cubic particles. For the procedure (iii), irregularly shaped particles, likely amorphous solid, were observed without any cubic particles. The product obtained from the procedure (iv) was the mixture of layered materials and cubic zeolite-like particles.

For the synthesis of zeolite-like materials with Zn in the frameworks, the formation of the homogeneous mixture of Zn and Si species is crucial to form the zincosilicate structures while preventing the precipitation of zinc oxides/hydroxides during hydrothermal treatment.[25] In the procedure (i), Zn species are totally dissolved as $[Zn(OH)_4]^{2-}$ or $[Zn(OH)_3]^{-}$ in the clear solution because of the high alkalinity of TMAdaOH solution (pH > 14).[26] The negatively charged Zn species can interact with $TMAda^+$, thereby preventing the precipitation of Zn even in such a highly alkaline solution. Separately, fumed silica particles are dispersed in the LiOH solution, yielding a semitransparent suspension (pH 12.5). When the Zn solution is mixed with the silica suspension, pH of the mixture drops to ca. 13, in which the solubility of Zn decreases.[26] Similar to aluminosilicates,[27] we surmise that the dissolved Zn species react with dissolved silicate, forming zincosilicate, and/or precipitate on the surface of dispersed silica particles. As a result, Zn and Si species are well mixed before hydrothermal treatment. In the procedure (ii), fumed silica is not dispersed beforehand; therefore, when it is added to the Zn solution, the reactions between dissolved Zn species and silica are restricted only at the external surface of agglomerated silica particles. The large amount of the unreacted silica would hence lead to the formation of layered silicate after hydrothermal treatment.

To further explain the difference between the procedures (i) and (ii), the intermediate products during hydrothermal treatment were recovered and characterized by UV-vis spectroscopy. As shown in Figure 2, only the product prepared via the procedure (ii) collected after 2 days exhibited a marked absorption band at around 360 nm, assigned to the $O^{2-} \rightarrow Zn^{2+}$ ligand-to-metal charge transfer transition in ZnO. The ZnO observed in the initial stage is probably due to the formation of Zn-rich species precipitated apart from the silicate species in the procedure (ii).

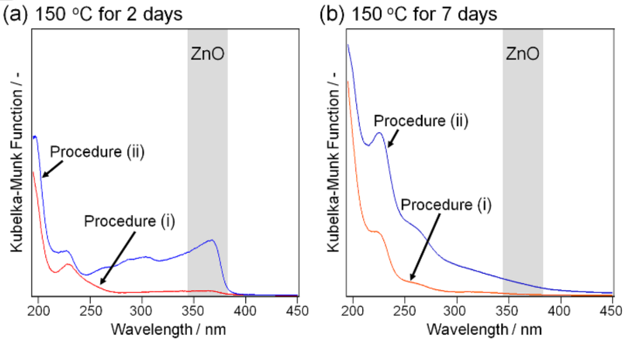

Figure 2. DR UV-Vis spectra of products collected after hydrothermal treatment at 150 °C for (a) 2 and (b) 7 days following procedures (i) and (ii).

In the procedure (iii), ZnO is formed immediately after addition of zinc acetate into the LiOH solution (pH 13), confirmed by XRD measurement (data not shown), because the solubility of Zn is somewhat low at this pH.[26,28] As a result, the reactions between Zn and Si species are limited. The procedure (iv) provides a weakly acidic, clear aqueous solution of Zn, in which Zn is present in the cationic Zn^{2+} form. When the acidic Zn solution is added to

10.1002/chem.201705277

the highly basic silica suspension (pH > 14), Zn is precipitated readily because of the rapid change in pH, yielding the inhomogeneous mixture of Zn and Si species. As a result, layered silicate and CHA are formed after hydrothermal treatment.

As shown in Figure S3 in the Supporting Information, by applying the successful procedure (i), effect of the types of alkali metal cation was investigated. When LiOH was replaced by NaOH or KOH, the CHA product was not obtained, even with the addition of seed crystals (pure silica CHA, 5 wt% based on SiO_2). In the absence of alkali metal cation, the CHA product was formed together with layered silicate when the seed crystals were added, while no crystalline product was observed without seed addition. These results suggest the important role of Li^+ on the formation of zincosilicate CHA, akin to the previous reports of zincosilicate *BEA and VET zeolite-like materials.[20,29]

Several synthetic parameters were examined to obtain zincosilicate CHA with varied Zn contents. As shown in Figure S4 in the Supporting Information, when the amount of Zn in the synthetic mixture was decreased to Si/Zn = 40, distinct XRD peak from layered silicate was observed, while peaks from CHA structure were hardly seen. However, when pure silica CHA was added as seed crystals, the formation of CHA product was confirmed at Si/Zn = 40. When the amount of Zn was further decreased to Si/Zn = 50, however, highly crystalline CHA product was not formed. Given the targeted use of zincosilicates for stabilization of multivalent cations, the Zn content in the synthetic mixture was also increased. The formation of CHA product was observed together with the unknown phase both with and without seed crystals when Si/Zn = 25. The formation of such impurity can be suppressed by carrying out the hydrothermal treatment under a tumbling condition (see Figure S5 in the Supporting Information).

Chemical compositions of the selected products are summarized in Table 1. The molar Si/Zn ratios of the CHA products were lower than those of the initial synthetic mixture, especially in the case of Zn-CHA1, which is likely because the solid product had low yield due to the absence of seed crystals. Nitrogen physisorption analysis confirms that all of the obtained zincosilicates had high micropore volumes. Thermogravimetric analysis shows that about 2.8 $TMAda^+$ cations were occluded in a unit cell of CHA structure, equivalent to 0.93 $TMAda^+$ per *cha* cage (Figure S6 in the Supporting Information). Note that the sharp weight loss due to $TMAda^+$ cation was not observed in the product synthesized by the procedure (ii).

Table 1. Chemical compositions, solid yields and micropore volumes of the obtained zincosilicate CHA products.

Sample	Seed[a] [wt%]	Condition	Reactant Si/Zn	Product Si/Zn[b]	Yield[c] [%]	V_{micro}[d] [$cm^3\ g^{-1}$]
Zn-CHA1	0	Static	33	12.8	47	0.24
Zn-CHA2	5	20 rpm	25	18.2	63	0.25
Zn-CHA3	5	20 rpm	20	14.5	70	0.25

[a] Pure silica CHA. [b] Determined by ICP-AES. [c] Calculated based on oxides. [d] Micropore volumes calculated by a *t*-plot method.

The incorporation of Zn into the zeolite framework was confirmed by the peak shifting toward lower angles in XRD patterns, compared to pure silica CHA (Figure 3). By assuming all products possess the same space group of $R\bar{3}m$, the cell parameters were calculated to be $a = b = 13.49$ Å and $c = 14.82$ Å for pure silica CHA ($R_{wp} = 0.109$, $R_p = 0.0854$), and $a = b = 13.55$ Å and $c = 14.97$ Å for Zn-CHA1 ($R_{wp} = 0.116$, $R_p = 0.0857$). As the Zn–O bond length (ca. 2 Å) is longer than the Si–O (ca. 1.6 Å), the lattice expansion clearly suggests the successful formation of CHA products with Zn in the framework.

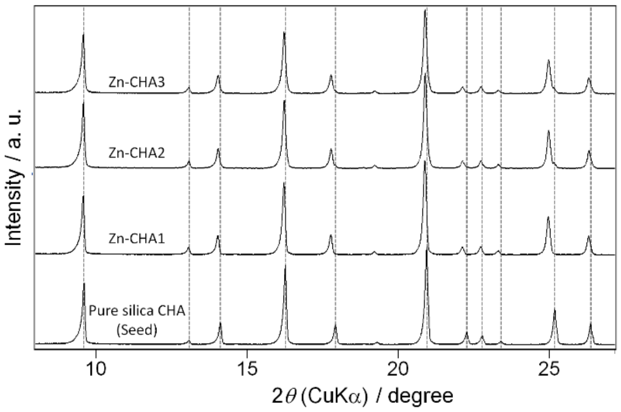

Figure 3. Comparison of powder XRD patterns of CHA products with various Zn contents.

As reported recently, zincosilicate zeolite-like materials show strong Lewis acidity.[25,30,31] FT-IR analysis of Zn-CHA2 after adsorption of deuterated acetonitrile (CD_3CN) at 80 °C and then desorbed at 80–250 °C was performed to characterize its Lewis acid sites in comparison with zincoaluminosilicate CHA[21] (Zn,Al-CHA; Si/Al = 10.5, Si/Zn = 15.3) (see Figures S8 and S9, and Table S1 in the Supporting Information). As shown in Figure S7a in the Supporting Information, the absorption band due to physisorbed CD_3CN was observed at 2267 cm^{-1}, while the band at ca. 2284 cm^{-1} is probably associated with Li-bearing Zn sites.[30] The bands present at 2308 and 2319 cm^{-1} are associated with CD_3CN coordinated to Lewis acid sites.[25,30] The existence of these two absorption bands suggests that there were two different Lewis acid sites in the zincosilicate CHA product, as the metal-substituted zeolite-like materials are known to have different metal sites, so-called “closed” and “open” sites (see Scheme 1).[30–33] The closed Zn site (observed at 2308 cm^{-1}) creating two negative charges is suitable for stabilization of bare divalent metal cations,[15,25] while the open Zn site (observed at 2319 cm^{-1}), a monocation ion-exchangeable site, has been considered as an active Lewis acid.[30,31] The Zn,Al-CHA sample also showed similar spectra; however, the band assigned to the Li-bearing sites at 2284 cm^{-1} observed in Zn-CHA2 was shifted to 2277 cm^{-1}, which is likely associated with Na^+ present in the Zn,Al-CHA sample (see Figure S7b in the Supporting Information).[30] While in the case of relating stannosilicates (well known as a Lewis acid

10.1002/chem.201705277

catalyst), most of adsorbed CD_3CN is desorbed upon evacuation at room temperature,[32] in both Zn-containing CHA samples CD_3CN remains on samples even after evacuation at 250 °C, suggesting the stronger Lewis acidity of zincosilicate materials.

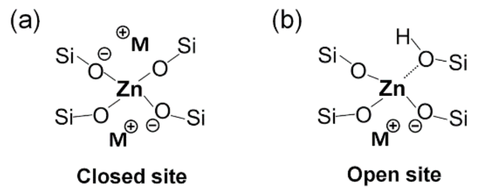

Scheme 1. Local structures of two different Zn sites: (a) closed site and (b) open site (M+ is a monovalent cation).

The ion-exchange ability of the zincosilicate CHA products was investigated for both monovalent and divalent cations in comparison with aluminosilicate (SSZ-13; Si/Al = 13.2) and zincoaluminosilicate[21] (Zn,Al-CHA) CHA materials (see Figures S8 and S9, and Table S1 in the Supporting Information). K^+ and Ni^{2+} cations were used as model monovalent and divalent cations, respectively. As shown in Figure 4a, the aluminosilicate SSZ-13 zeolite reached 86% ion-exchange efficiency after 48 h. In contrast, the zincosilicate CHA products exhibited slower ion-exchange rate and the ion-exchange efficiency became 31% for Zn-CHA1 (Si/Zn = 12.8) and 52% for Zn-CHA2 (Si/Zn = 18.2) after 48 h. Note that the ion-exchange efficiency was calculated by assuming that all Zn in the framework generate two negative charges per Zn atom (i.e., closed Zn sites). This slower rate may be due to the larger particle sizes of the zincosilicate CHA products and the structure constrain arising from the high density of the negative charges in the structures

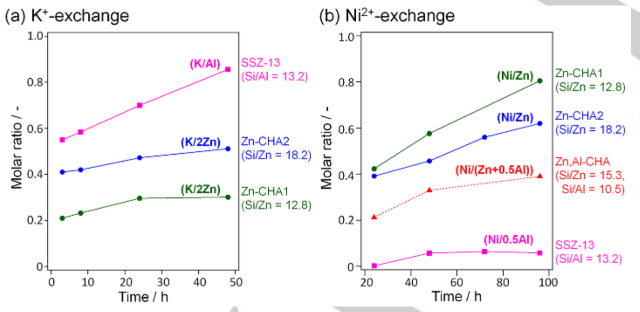

Figure 4. Contents of ion-exchange versus time of (a) K^+ and (b) Ni^{2+} cations for zincosilicate, aluminosilicate (SSZ-13) and zincoaluminosilicate CHA samples.

The benefit of Zn in the zeolite framework for ion-exchange of divalent cations was demonstrated using Ni^{2+} because Ni^{2+}-exchanged zeolites and zeolite-like materials are promising catalysts for dimerization and oligomerization of olefins.[15,34] As shown in Figure 4b, the SSZ-13 sample showed very low ion-exchange efficiency (only 6% after 96 h). The formation of the paired Al sites is known to be unfavorable in the case of SSZ-13 zeolite due to the high charge density of $TMAda^+$ employed for its synthesis.[16] As a result, the SSZ-13 sample used here is not suitable for ion-exchange of divalent cations. On the contrary, the zincosilicate CHA products exhibited higher ion-exchange efficiency (80% and 62% after 96 h for Zn-CHA1 and Zn-CHA2, respectively) despite the fact that the zincosilicate CHA products have comparable substitution contents to that of aluminosilicate SSZ-13 (i.e., similar Si/Zn and Si/Al ratios). The zincoaluminosilicate CHA[21] has intermediate ion-exchange efficiency (39% after 96 h), suggesting that Zn in the zincoaluminosilicate framework can stabilize Ni^{2+}, while the content of the paired Al sites is insufficient for the divalent cation-exchange.

FT-IR spectra of Zn-CHA2 before and after ion-exchange with Ni^{2+} are depicted in Figure S10 in the Supporting Information. The disappearance of the broad band centered at 3630 cm^{-1}, presumably assigned to the bridging SiOHZn groups, after ion-exchange confirmed the ion-exchange from protons to Ni^{2+}. In addition, no marked absorption band due to the Ni–OH vibration, typically appearing at around 3640 cm^{-1},[35] was observed, suggesting that no significant amount of $Ni(OH)^+$ species was formed after ion-exchange. Effect of thermal treatment on the environment of Ni^{2+} species was investigated. After ion-exchange for 96 h, DR UV-vis spectra of the Ni^{2+}-exchanged Zn-CHA2 (Ni/Zn = 0.62) and Zn,Al-CHA (Ni/(Zn+0.5Al) = 0.39) samples showed characteristic absorption bands correlated to Ni^{2+} cations in octahedral symmetry,[36] suggesting the presence of $[Ni(H_2O)_6]^{2+}$ complexes in the samples (Figure S11a in the Supporting Information). After thermal treatment under dried air at 600 °C for 6 h, both Zn-CHA2 and Zn,Al-CHA samples exhibited additional bands at around 260 nm (Figure S11b in the Supporting Information), attributed to an electronic transition with charge transfer (CT) in NiO.[37] The position of this $O^{2-} \rightarrow Ni^{2+}$ CT band is related to the degree of agglomeration of NiO species (note that the CT band for bulk NiO is observed at 320 nm).[37] The blue shift of this band observed in both samples suggests the formation of small NiO clusters.[37] The band observed in Zn,Al-CHA was stronger than that in Zn-CHA2 and had a broad shoulder between 260 and 350 nm, suggesting the higher degree of NiO agglomeration (i.e., larger clusters). Collectively, these results suggest that the zincosilicate CHA products were superior to the aluminosilicate and zincoaluminosilicate counterparts for ion-exchange and stabilization of divalent cations such as Ni^{2+}.

In summary, microporous zincosilicate CHA materials were synthesized for the first time with a particular focus on the mixing procedures of the raw materials, yielding CHA products with varied Zn contents (Si/Zn = 12.8–18.2). Control of the initial state of Zn species was found to be very crucial to prevent the precipitation of zinc oxides/hydroxides, the formation of extraframework Zn species, and the formation of impure phases. The obtained zincosilicate CHA products possessed remarkably higher ion-exchange ability for divalent cations, demonstrated using Ni^{2+}, compared to that of aluminosilicate and zincoaluminosilicate counterparts.

Acknowledgements

This work was supported in part by JSPS through a Grant-in-Aid for Young Scientists (B) (KAKENHI: 16K18284) and the Asahi Glass Foundation. We thank Prof. M. Ogura (The University of Tokyo) for the access to an FT-IR instrument. N. K. is a JSPS research fellow (DC 2) and has received financial support from JSPS and the Program for Leading Graduate Schools, “Global Leader Program for Social Design and Management”, by MEXT.

Keywords: Hydrothermal synthesis • Ion exchange • Nickel • Zeolites • Zincosilicates

[1] M. A. Snyder, M. Tsapatsis, *Angew. Chem.* **2007**, *119*, 7704–7717; *Angew. Chem. Int. Ed.* **2007**, *46*, 7560–7573.
[2] W. Chaikittisilp, T. Okubo in *Handbook of Solid State Chemistry*, *Vol. 4* (Eds.: R. Dronskowski, S. Kikkawa, A. Stein), Wiley-VCH Verlag GmbH & Co. KGaA, Weinheim, **2017**, pp. 97–119.
[3] M. Moliner, C. Martínez, A. Corma, *Chem. Mater.* **2014**, *26*, 246–258.
[4] P. Tian, Y. Wei, M. Ye, Z. Liu, *ACS Catal.* **2015**, *5*, 1922–1938.
[5] W. Dai, X. Sun, B. Tang, G. Wu, L. Li, N. Guan, M. Hunger, *J. Catal.* **2014**, *314*, 10–20.
[6] R. Zhang, N. Liu, Z. Lei, B. Chen, *Chem. Rev.* **2016**, *116*, 3658–3721.
[7] C. Paolucci, J. R. Di Iorio, F. H. Ribeiro, R. Gounder, W. F. Schneider, *Adv. Catal.* **2016**, *59*, 1–107.
[8] B. E. R. Snyder, P. Vanelderen, M. L. Bols, S. D. Hallaert, L. J. Böttger, L. Ungur, K. Pierloot, R. A. Schoonheydt, B. F. Sels, E. I. Solomon, *Nature* **2016**, *536*, 317–321.
[9] S. Grundner, M. A. C. Markovits, G. Li, M. Tromp, E. A. Pidko, E. J. M. Hensen, A. Jentys, M. Sanchez-Sanchez, J. A. Lercher, *Nat. Commun.* **2015**, *6*, 7546.
[10] C. Paolucci, A. A. Parekh, I. Khurana, J. R. Di Iorio, H. Li, J. D. A. Caballero, A. J. Shih, T. Anggara, W. N. Delgass, J. T. Miller, F. H. Ribeiro, R. Gounder, W. F. Schneider, *J. Am. Chem. Soc.* **2016**, *138*, 6028–6048.
[11] P. Tomkins, M. Ranocchiari, J. A. van Bokhoven, *Acc. Chem. Res.* **2017**, *50*, 418–425.
[12] Y. Kuroda, M. Iwamoto, *Top. Catal.* **2004**, *28*, 111–118.
[13] J. Dědeček, Z. Sobalík, B. Wichterlová, *Catal. Rev.* **2012**, *54*, 135–223.
[14] J. Dědeček, L. Čapek, P. Sazama, Z. Sobalík, B. Wichterlová, *Appl. Catal. A* **2011**, *391*, 244–253.
[15] M. A. Deimund, J. Labinger, M. E. Davis, *ACS Catal.* **2014**, *4*, 4189–4195.
[16] J. R. Di Iorio, R. Gounder, *Chem. Mater.* **2016**, *28*, 2236–2247.
[17] C. C. Freyhardt, R. F. Lobo, S. Khodabandeh, J. E. Lewis, Jr., M. Tsapatsis, M. Yoshikawa, M. A. Camblor, M. Pan, M. M. Helmkamp, S. I. Zones, M. E. Davis, *J. Am. Chem. Soc.* **1996**, *118*, 7299–7310.
[18] C. Röhrig, H. Gies, *Angew. Chem.* **1995**, *107*, 125–127; *Angew. Chem. Int. Ed. Engl.* **1995**, *34*, 63–65.
[19] Y. Suzuki, T. Wakihara, S. Kohara, K. Itabashi, M. Ogura, T. Okubo, *J. Phys. Chem. C.* **2011**, *115*, 443–446.
[20] D. P. Serrano, R. van Grieken, M. E. Davis, J. A. Melero, A. Garcia, G. Morales, *Chem. Eur. J.* **2002**, *8*, 5153–5160.
[21] M. J. Dusselier, M. E. Davis, U.S. Pat. Appl. 20160243531A1, **2016**.
[22] S. I. Zones, R. A. Van Nordstrand, *Zeolites* **1988**, *8*, 166–174.
[23] E. A. Eilertsen, S. Bordiga, C. Lamberti, A. Damin, F. Bonino, B. Arstad, S. Svelle, U. Olsbye, K. P. Lillerud, *ChemCatChem* **2011**, *3*, 1869–1871.
[24] J. W. Harris, W.-C. Liao, J. R. Di Iorio, A. M. Henry, T.-C. Ong, A. Comas-Vives, C. Copéret, R. Gounder, *Chem. Mater.* **2017**, *29*, 8824–8837.
[25] N. Koike, W. Chaikittisilp, K. Iyoki, Y. Yanaba, T. Yoshikawa, S. P. Elangovan, K. Itabashi, T. Okubo, *Dalton Trans.* **2017**, *46*, 10837–10846.
[26] A. J. B. Dutra, P. R. P. Paiva, L. M. Tavares, *Miner. Eng.* **2006**, *19*, 478–485.
[27] T. Ikuno, W. Chaikittisilp, Z. Liu, T. Iida, Y. Yanaba, T. Yoshikawa, S. Kohara, T. Wakihara, T. Okubo, *J. Am. Chem. Soc.* **2015**, *137*, 14533–14544.
[28] R. A. McBride, J. M. Kelly, D. E. McCormack, *J. Mater. Chem.* **2003**, *13*, 1196–1201.
[29] M. Yoshikawa, S. I. Zones, M. E. Davis, *Microporous Mater.* **1997**, *11*, 127–136.
[30] M. Orazov, M. E. Davis, *Chem. Sci.* **2016**, *7*, 2264–2274.
[31] R. E. Patet, S. Caratzoulas, D. G. Vlachos, *J. Phys. Chem. C* **2017**, *121*, 22178–22186.
[32] M. Boronat, P. Concepción, A. Corma, M. Renz, S. Valencia, *J. Catal.* **2005**, *234*, 111–118.
[33] P. Wolf, M. Valla, A. J. Rossini, A. Comas-Vives, F. Núñez-Zarur, B. Malaman, A. Lesage, L. Emsley, C. Copéret, I. Hermans, *Angew. Chem.* **2014**, *126*, 10343–10347; *Angew. Chem. Int. Ed.* **2014**, *53*, 10179–10183.
[34] R. Y. Brogaard, U. Olsbye, *ACS Catal.* **2016**, *6*, 1205–1214.
[35] G. Kinger, A. Lugstein, R. Swagera, M. Ebel, A. Jentys, H. Vinek, *Microporous Mesoporous Mater.* **2000**, *39*, 307–317.
[36] C. Lepetit, M. Che, *J. Phys. Chem.* **1996**, *100*, 3137–3143.
[37] R. A. Ortega-Domínguez, H. Vargas-Villagrán, C. Penaloza-Orta, K. Saavedra-Rubio, X. Bokhimi, T. E. Klimova, *Fuel* **2017**, *198*, 110–122.

Entry for the Table of Contents

Layout 1:

COMMUNICATION

Catching Two Charges. Microporous zincosilicates with CHA topology are synthesized for the first time with a particular focus on the mixing procedures of the raw materials. The resulting zincosilicate materials show remarkably high ion-exchange ability for divalent cations, compared to their aluminosilicate and zincoaluminosilicate analogs.

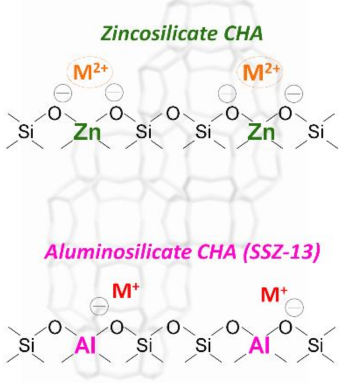

N. Koike, K. Iyoki, S. H. Keoh, W. Chaikittisilp, T Okubo**

Page No. – Page No.

Synthesis of a New Microporous Zincosilicate with CHA Zeolite Topology as Efficient Platforms for Ion-Exchange of Divalent Cations